Journal of
Plankton Research

plankt.oxfordjournals.org

*J. Plankton Res.* (2016) 38(4): 1052–1061. First published online January 18, 2016 doi:10.1093/plankt/fbv120

Contribution to the Themed Section: Scaling from individual plankton to marine ecosystems

# Diel variability in the elemental composition of the marine cyanobacterium *Synechococcus*

**JOHANN S. LOPEZ[1], NATHAN S. GARCIA[1]*, DAVID TALMY[2] AND ADAM C. MARTINY[1,3]**

[1]DEPARTMENT OF EARTH SYSTEM SCIENCE, UNIVERSITY OF CALIFORNIA, IRVINE, CA, USA, [2]DEPARTMENT OF EARTH, ATMOSPHERE AND PLANETARY SCIENCES, MASSACHUSETTS INSTITUTE OF TECHNOLOGY, CAMBRIDGE, MA, USA AND [3]DEPARTMENT OF ECOLOGY AND EVOLUTIONARY BIOLOGY, UNIVERSITY OF CALIFORNIA, IRVINE, CA, USA

*CORRESPONDING AUTHOR: n8garcia@gmail.com

Received August 26, 2015; accepted December 10, 2015

Corresponding editor: Pia Moisander

The ratio of elements such as carbon:nitrogen:phosphorus (C:N:P) in phytoplankton is known to vary substantially within single isolates and across environmental gradients. In addition, C:N:P is known to vary throughout the day due to diel patterns in nutrient acquisition and storage. It has been hypothesized that small phytoplankton such as marine cyanobacteria have relatively invariable elemental ratios during a 24 h period, whereas larger phytoplankton have a greater capacity to store elements and thus a wider diel range of C:N:P. To test this hypothesis, we examined diel variability in cellular C:N:P, using a chemostat culturing system, for one of the most abundant marine cyanobacteria, *Synechococcus* (WH8102) during two 24 h periods. The cellular C quota nearly doubled during the 14 h light period and was subsequently reduced during the dark period. The cellular N quota also varied considerably, whereas the P quota remained relatively stable. These daily changes in elemental quotas led to highly variable $C{:}N_{cell}$ and $C{:}P_{cell}$. Furthermore, the magnitude of variability in cellular elemental stoichiometry of *Synechococcus* was positively related to the growth rate. We constructed a model to test the extent to which variation in $C{:}N_{cell}$ and $C{:}P_{cell}$ is related to reserve carbon accumulation and depletion over each light–dark cycle. Results imply that, in addition to growth-related respiratory losses, *Synechococcus* also purges excess C during the dark period in order to maintain a nutritive balance within cells. Our data suggest that diel variation in $C{:}N_{cell}$ and $C{:}P_{cell}$ of *Synechococcus* is of the same order of magnitude as stoichiometric variation within plankton communities between major ocean environments.

KEYWORDS: cyanobacteria; *Synechococcus*; stoichiometry; diel; Redfield; phytoplankton

## INTRODUCTION

In the 80 years since its inception, the identification of a nearly constant, atomic C:N:P ratio in the marine environment has remained a central foundation of marine biogeochemical processes (Redfield, 1958). Despite substantial plasticity in cellular C:N:P in both field and laboratory observations (Karl *et al.*, 2001; Bertilsson *et al.*, 2003; Heldal *et al.*, 2003), fixed elemental stoichiometry in marine phytoplankton has been consistently used to infer global primary production (Martin *et al.*, 1987), carbon export (Krishnamurthy *et al.*, 2009) and nitrogen fixation and loss rates (Deutsch *et al.*, 2001, 2007). More recent observations and models indicate that the elemental stoichiometry of marine particles varies between vast N- and P-limited ocean basins and regions (Martiny *et al.*, 2013a,b; DeVries and Deutsch, 2014; Teng *et al.*, 2014). The mechanisms that drive variation in elemental stoichiometry have been attributed to nutrient-limited growth (Rhee, 1978; McCarthy and Goldman, 1979; Sterner and Elser, 2002), light (Laws and Bannister, 1980; Urabe *et al.*, 2002), temperature (Toseland *et al.*, 2013) and taxonomy (Geider and La Roche, 2002; Ho *et al.*, 2003; Weber and Deutsch, 2010; Quigg *et al.*, 2011; Martiny *et al.*, 2013a). Thus, environmental controls on basic growth physiology and community composition of marine phytoplankton contribute to spatial and temporal patterns in elemental stoichiometry of marine biota (Flombaum *et al.*, 2013, Martiny *et al.*, 2013a).

In addition to broad spatial and temporal patterns, elemental stoichiometry of phytoplankton is known to vary in short daily rhythms within cells (Geider and La Roche, 2002; Granum *et al.*, 2002; Talmy *et al.*, 2014). For example, the marine cyanobacterium *Crocosphaera watsonii* separates inorganic C and $N_2$ fixation during the day and night (Berman-Frank *et al.*, 2007), leading to daily patterns in cellular C:N ratios (Mohr *et al.*, 2010; Saito *et al.*, 2011; Gradoville *et al.*, 2014). In chemostat cultures of the diatom *Skeletonema costatum*, cellular carbon cycling during light and dark periods was shown to confer a daily pattern in C:N (Anning *et al.*, 2000). In contrast, small phytoplankton such as *Prochlorococcus* and *Synechococcus* have been suggested to have a smaller capacity to store C and N and therefore a relatively invariable C:N ratio (Talmy *et al.*, 2014) when compared with large phytoplankton such as diatoms. This stronger flexibility in large cells may lead to a competitive advantage in terms of energy storage and growth in environments in which the light intensity is highly variable, such as in deeply mixed layers, or in which the light period is short, as it can be in high latitude waters (Van Oijen *et al.*, 2003).

Specific cell components can create diel variability in elemental stoichiometry of phytoplankton (Geider and La Roche, 2002). For example, some studies report diel variability in nucleic acid concentrations and pigment fluorescence of *Prochlorococcus* and *Synechococcus* (Vaulot *et al.*, 1995; Jacquet *et al.*, 2001). Other data indicate that amino acid uptake has a diel pattern (Mary *et al.*, 2008), which is likely synchronous with cellular protein concentrations (Matallana-Surget *et al.*, 2014). Cycling of cellular pools containing a high C:P ratio (e.g. proteins and carbohydrates) relative to those with a low C:P ratio (e.g. nucleic acids and polyphosphates) could also create diel variability in cellular elemental stoichiometry.

In order to determine how cellular elemental stoichiometry varies over a diel period in small phytoplankton, we first asked how does cellular C, N and P content in steady-state chemostat cultures of *Synechococcus* WH8102 change over two 24 h periods. Secondly, we asked how differences in the growth rate contribute to diel variability in elemental stoichiometry. Thirdly, using a mathematical model, we identify putative physiological mechanisms that contribute to this variability. *Synechococcus* contributes to a large fraction of net ocean primary production (Flombaum *et al.*, 2013) and thus plays a major role in cycling of biogeochemical elements. Fine-scale resolution of elemental stoichiometry in dominant lineages of marine plankton is needed to more accurately model marine biogeochemical processes (Prézelin, 1992).

## METHOD

Chemostat cultures of *Synechococcus* (WH8102) were grown in 8 L-polycarbonate bottles at 24°C. Ambient light (195 μmol quanta $m^{-2}$ $s^{-1}$) was supplied using cool white fluorescent lamps on a 14:10 light:dark cycle (Mouginot *et al.*, 2015). We selected the temperature and light conditions on the basis of optimal growth conditions reported by Mackey *et al.* (2013) and Moore *et al.* (1995). All parts of the chemostat system were autoclaved before adding ~60 mL inoculum culture of *Synechococcus* over an open flame to minimize biological contamination. The culture medium (artificial seawater) was autoclaved and cooled to room temperature before adding 0.2 μm-filtered bicarbonate, carbonate, nitrate, phosphate and trace metals in concentrations described by Garcia *et al.* (in review) to limit biomass accumulation by nitrate (added as $NaNO_3$), where measured nutrient concentrations in the medium were 15.9 μM $NO_3^-$ and 9.2 μM $PO_4^{3-}$ (added as $K_2HPO_4$; $N{:}P_{input} = 1.7$). Phosphate and nitrate concentrations were measured with the colorimetric assay, described in the Bermuda Atlantic Time-series Study protocols (Michaels *et al.*, 1997a, b) using a ThermoVis 2000 spectrophotometer at 885 and 543 nm, respectively. We selected these specific sources of N and P because of their prominence throughout

the world's oceans. All parts used to culture *Synechococcus* were autoclaved, and transfer of media and cultures to the chemostat system was performed in a laminar flow hood over an open flame. The culturing system was sealed with 0.2 μm-filtered air pumped into the chamber and a 0.2 μm filter attached to an air outlet. Dilution rates (i.e. growth rates) were controlled by modulating the culture volume (2.3–5.25 L) rather than the flow rate.

We collected samples for elemental ratio estimates and cell measurements (1 mL) from steady-state cultures every 3 h during two 24 h periods. The second 24 h period was measured 7 days after the first period. Culture samples for the analysis of particulate organic carbon and nitrogen (POC and PON; 150 mL) and particulate organic phosphorus (POP; 50 mL) were passed through pre-combusted (450°C) GF/F Whatman glass fiber filters under low pressure (5 psi). Samples for the analysis of POC and PON were dried at 60–80°C (~48 h), pelletized and analyzed using an EA CN Elemental Analyzer (Thermo-Scientific). Samples were rinsed with 0.17 M $NaSO_4$, and samples for POP analysis were then dried at 60–80°C with 2 mL of 0.017 M $MgSO_4$ and combusted at 450°C for 2 h before adding 5 mL 0.2 M HCl and baking at 80–90°C. The resulting orthophosphate concentrations were measured using the Bermuda Atlantic Time-series Study protocols (Michaels *et al.*, 1997a). We analyzed the culture cell density with a flow cytometer (Accuri C6) by identifying particles with forward scatter (FSCH) and Chl *a* fluorescence. We also measured the fluorescence of phycoerythrin with the flow cytometer. A script was then used in MATLAB (The MathWorks, Inc., Natick, MA, USA) to fit a least-squares sine function to cell quota data for each growth rate treatment (Fig. 1).

Although we do not have direct measurements of heterotrophs from our chemostats, other estimates suggest that heterotrophic contaminants represent a small portion of the total biomass of our *Synechococcus* cultures. In chemostat cultures grown under nearly identical conditions, the number of fluorescent cells was always >90% of all particles visible with light microscopy at 40×. In addition, we have good agreement between estimates of stoichiometry in the data reported here and elsewhere, where we monitored chemostats with fluorescence microscopy (Garcia *et al.*, in review).

To explore the influence of reserve carbon accumulation and depletion on stoichiometric variation over a diurnal cycle, we used a model that connects organism growth rate with carbon fixation and protein synthesis. A full model description is provided in the Supplementary data. The model structure and main assumptions are similar to previously published model forms (Geider *et al.*, 1998; Flynn, 2008; Talmy *et al.*, 2014). We built on previous models by exploring various assumptions regarding

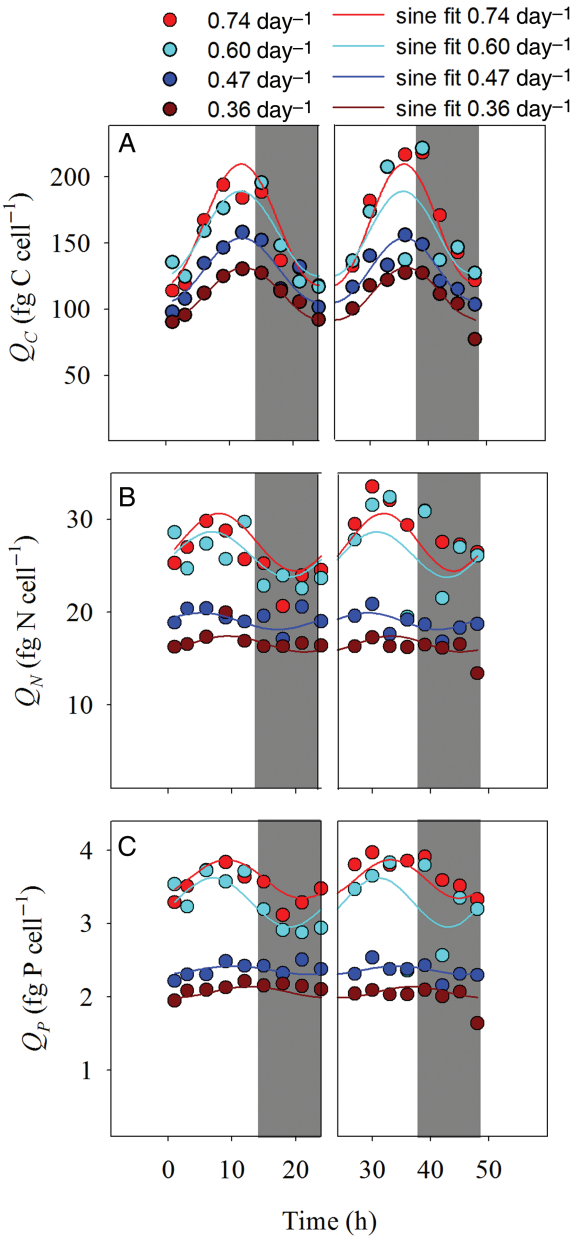


**Fig. 1.** Diel cycling of cellular carbon ($Q_C$, **A**), nitrogen ($Q_N$, **B**) and phosphorus ($Q_P$, **C**) content as a function of steady-state growth in nitrate-limited chemostat cultures of *Synechococcus*. Gray bands indicate dark periods during two 24 h periods. Break in *x*-axis denotes 7-day period between first and second 24 h sampling period. Sine curves were best fit to the data using a least-squares script.

the day–night dependence of the carbon loss rate and considered the implications of our findings for understanding the ecology of *Synechococcus*. For all simulations, the nutrient concentration in the input reservoir ($S_{in}$) and the dilution rate ($D$) exactly matched the experimental conditions. With this design, we tested the influence of two contrasting assumptions on the model dynamics: (i) growth-rate-independent carbon losses, which may include maintenance respiration

and excretion, are equal to 0.01 $day^{-1}$ and thus have a negligible influence on diurnal changes in elemental stoichiometry and (ii) a preferential purging of carbon by *Synechococcus* (4.0 $day^{-1}$) in a manner that is independent of growth rate. Furthermore, carbon losses are assumed to be negligible in the day (0.01 $day^{-1}$), but elevated at night (Supplementary data, Table SII).

## RESULTS

To examine diel patterns in cellular elemental stoichiometry, we grew *Synechococcus* (WH8102) in chemostat cultures, limiting biomass accumulation with a low supply of nitrate ($N{:}P_{input} = 1.7$). We analyzed cellular elemental quotas during two 24 h periods and observed a strong daily pattern in the cellular carbon and nitrogen quotas ($Q_C$ and $Q_N$) (Fig. 1). This included substantial (up to 93%) increases during the light period and decreases during the dark period. The percent change in $Q_C$ and $Q_N$ during the day scaled positively with increasing growth rate (Fig. 1). In the fast-growing culture (0.74 $day^{-1}$), $Q_C$ increased by 93% (increasing from 113 to 218 fg C $cell^{-1}$), whereas $Q_N$ only increased by 50% (20–31 fg N $cell^{-1}$; Table I and Fig. 1). In the slowest growing culture, however, $Q_C$ only increased by 44% (from 90 to 130 fg C $cell^{-1}$), whereas $Q_N$ increased by 7% (16–17 fg N $cell^{-1}$; Table I and Fig. 1). Changes in the cellular phosphorus quota ($Q_P$) were similar, but percent increases during the day were generally smaller, increasing by 27% (3.12–3.96 fg P $cell^{-1}$) in the fast-growing culture (0.74 $day^{-1}$) and 13% in the slow-growing culture (0.36 $day^{-1}$; Table I and Fig. 1). Cell size was monitored independently with flow cytometry as FSCH (a proxy for cell size based on cell diameter) and revealed a pattern similar to that of $Q_C$; the cell size was highly correlated with $Q_C$ ($R = 0.93$, $P < 0.001$; Fig. 2). Thus, the range of variation in $Q_C$ and cell size over the diel cycle scaled positively with growth, and the largest differences between cultures were observed at the conclusion of the light period. $Q_N$ and $Q_P$, however, exhibited peaks

*Table I: Lowest and highest cell quotas (fg $cell^{-1}$) and relative percent increases in cell quotas for each culture of* Synechococcus

| | | Observed data | | | Sine fit data | | |
|---|---|---|---|---|---|---|---|
| Cell quota | Growth rate ($day^{-1}$) | Lowest quota | Highest quota | Percent increase | Lowest quota | Highest quota | Percent increase |
| $Q_C$ | 0.74 | 113 (1) | 218 (39) | 93 | 118 (24) | 210 (36) | 78 |
| | 0.60 | 117 (24) | 221 (39) | 89 | 124 (24) | 177 (39) | 42 |
| | 0.47 | 98 (1) | 158 (12) | 61 | 105 (24) | 154 (36) | 47 |
| | 0.36 | 77 (48) | 130 (12) | 69 | 92 (24) | 132 (36) | 43 |
| $Q_N$ | 0.74 | 20 (18) | 31 (39) | 50 | 25 (21) | 31 (33) | 24 |
| | 0.60 | 23 (15) | 32 (33) | 42 | 24 (18) | 29 (30) | 20 |
| | 0.47 | 17 (18) | 21 (30) | 22 | 18 (18) | 20 (30) | 10 |
| | 0.36 | 16 (42) | 17 (3) | 6 | 16 (21) | 17 (33) | 10 |
| $Q_P$ | 0.74 | 3.12 (18) | 3.96 (30) | 27 | 3.35 (21) | 3.87 (33) | 16 |
| | 0.60 | 3.19 (15) | 3.83 (33) | 20 | 2.97 (18) | 3.61 (30) | 22 |
| | 0.47 | 2.16 (42) | 2.53 (30) | 18 | 2.31 (21) | 2.42 (33) | 5 |
| | 0.36 | 1.95 (1) | 2.21 (12) | 13 | 1.99 (1) | 2.14 (12) | 8 |

Timing (hour) of minima and maxima is in parentheses.

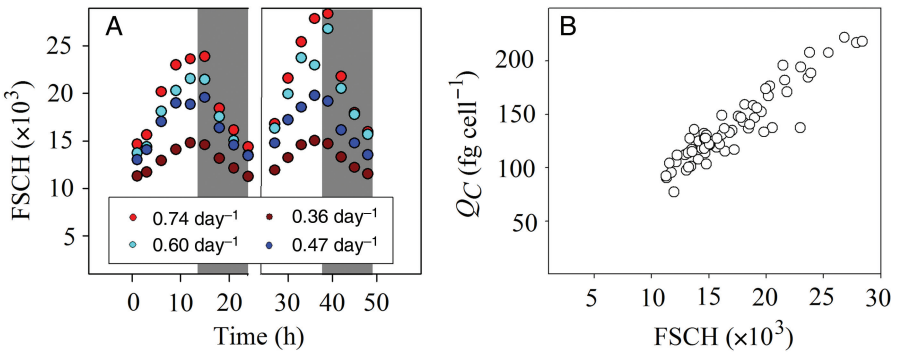


**Fig. 2.** (**A**) Diel cycling of forward scatter (FSCH, a proxy for cell size) as a function of steady-state growth and (**B**) relationship between FSCH data in (A) and $Q_C$ data in Fig. 1A in nitrate-limited chemostat cultures of *Synechococcus*. Gray bands indicate dark periods during two 24 h periods. Break in *x*-axis denotes 7-day period between first and second 24 h sampling period.

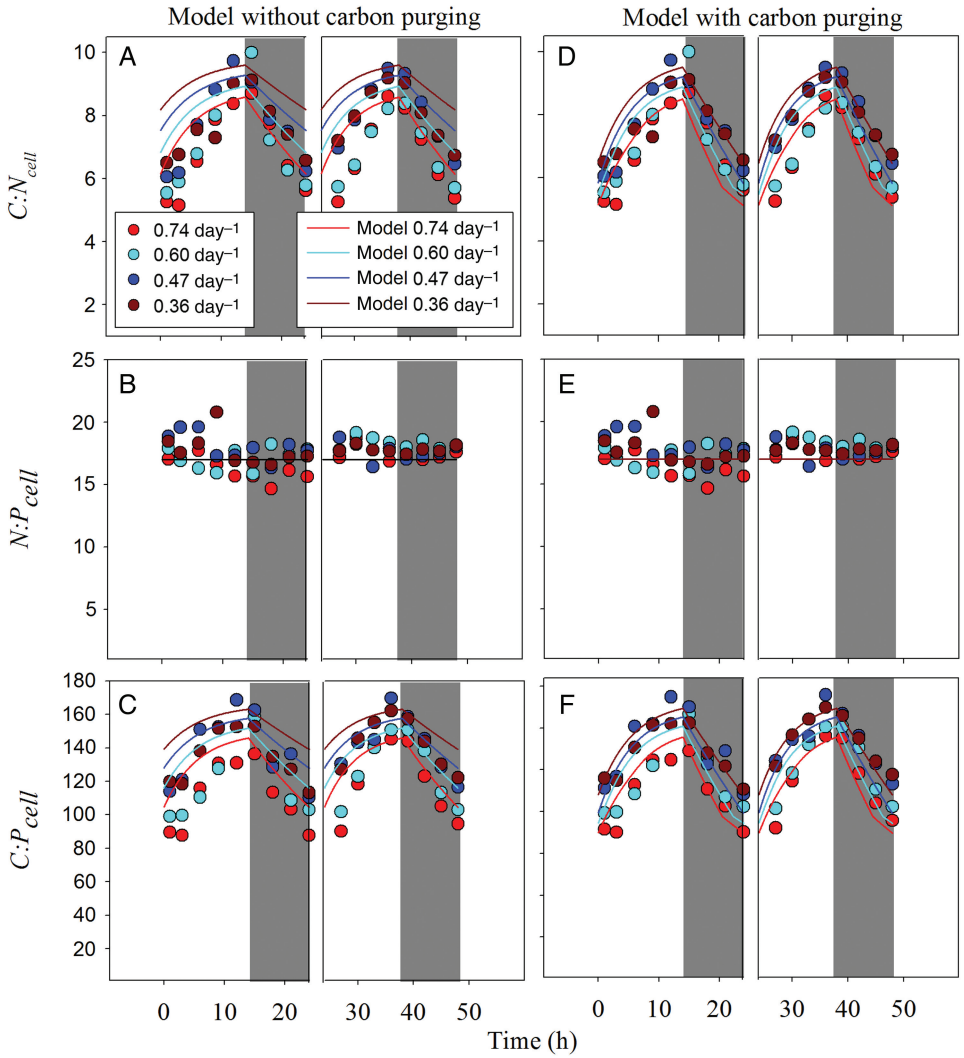


**Fig. 3.** Diel cycling of cellular elemental ratios: carbon: nitrogen (**A**), nitrogen: phosphorus (**B**) and carbon: phosphorus (**C**) as a function of steady-state growth in nitrate-limited chemostat cultures of *Synechococcus*. Gray bands indicate dark periods during two 24 h periods. Break in *x*-axis denotes 7-day period between first and second 24 h sampling period. Models of diel patterns in elemental stoichiometry as a function of the growth rate without (A–C) and with (**D–F**) carbon purging overlay on empirical data (see Methods and Supplementary data for model details).

roughly midway through the light period and troughs roughly midway through the dark period (Fig. 1B and C), particularly in the two fast-growing cultures. The sinusoidal spline interpolation through the $Q_N$ and $Q_P$ of these cultures confirmed that the maxima occurred ~8 h prior to the conclusion of the light period (Fig. 1B and C).

Diel variation in $Q_C$, $Q_N$ and $Q_P$ led to large oscillations in $C{:}P_{cell}$ and $C{:}N_{cell}$ (Table I and Fig. 3), which scaled positively with growth. Although diel ratios of $C{:}P_{cell}$ and $C{:}N_{cell}$ increased by 66% and 69% in the fast-growing culture (0.74 day$^{-1}$), respectively, diel ratios of $N{:}P_{cell}$ only increased by 20% (Table II). In the slow-growing culture (0.36 day$^{-1}$), percent changes in $C{:}P_{cell}$, $C{:}N_{cell}$ and $N{:}P_{cell}$ were smaller: 43%, 41% and 11%, respectively. Daily maximum values of $C{:}N_{cell}$ and $C{:}P_{cell}$ occurred at the end of the 14 h light period, leading to the hypothesis that daily carbon acquisition and losses were the main drivers of diel variation in cellular elemental stoichiometry of *Synechococcus*.

Pigment fluorescence data also exhibited diel variability with maxima ~8 h before the conclusion of the light period (Fig. 4A and B). Because the majority of the main pigment phycoerythrin is composed of nitrogen-rich proteins, we compared diel variability in $Q_N$ to variability in fluorescence of pigments (Fig. 4C and D). This apparent relation was analyzed by simple linear regression, and $Q_N$ was highly correlated with pigment fluorescence ($R = 0.92$, $P < 0.001$) with a coefficient of determination ($r^2$) of 0.85 for both phycoerythrin and Chl *a*.

To explore the functional cause of diurnal variation in *Synechococcus* elemental stoichiometry, a cellular model was parameterized to mimic the chemostat culture conditions [Supplementary data, Table SI, Equation (S1); Talmy *et al.*, 2014]. Our model was able to recapitulate the bimodal pattern that was observed for $C{:}N_{cell}$ and $C{:}P_{cell}$ over the course of two 24 h cycles (Fig. 3). Furthermore, our assumption of constant $N{:}P_{cell}$ during diel cycles yielded suitable fits to observations (Fig. 3B and E). Because cells were limited by N throughout the experiment, the intracellular concentration of reserve, inorganic nitrogen ($N_R$) and the N concentration in the chamber ($S$) were both low by comparison to all other modeled biomass variables ($C_R$,$N_F$,$C_F$ Table S2; data not shown). Thus, the stoichiometric variation observed in the model arises due to changes in the functional and structural apparatus and the carbon reserve.

We present results from our model using two contrasting assumptions regarding the carbon loss rate. First, when the main carbon loss is assumed to be a function of growth rate, the parameter $R$, which constrains growth-rate-independent carbon losses, was set to an arbitrarily low number for the duration of the experiment. With this assumption, the amplitude of $C{:}N_{model}$ and $C{:}P_{model}$ depends strongly on the dilution rate within the chamber (Fig. 3A and C). At the lowest dilution rates, the model overestimates $C{:}N_{cell}$ and $C{:}P_{cell}$ at dawn, which suggests that there is an additional night time loss of carbon, which is not accounted for in this configuration. In contrast, when we assumed a high night time loss of carbon (Supplementary data, Table SII) that is independent of growth rate [Supplementary data, Table SI, Equations (S3) and (S9)], the model produces a bimodal pattern in $C{:}N_{cell}$ and $C{:}P_{cell}$ with amplitude similar to the observational data, even for different dilution rates (Fig. 3D and F). Under this assumption, the $C{:}N_{model}$ and $C{:}P_{model}$ at dawn are much closer to the observed values (Fig. 3D and F). Thus, our model and data suggest that the carbon loss rate at night is high and could be due to respiration or carbon purging.

*Table II: Lowest value, highest value and relative increase in cellular elemental ratios for each culture of* Synechococcus

| Elemental ratios | Growth rate ($day^{-1}$) | Lowest value | Highest value | Percent increase |
|---|---|---|---|---|
| $C{:}N_{cell}$ | 0.74 | 5.15 | 8.69 | 69 |
| | 0.60 | 5.53 | 9.99 | 80 |
| | 0.47 | 6.05 | 9.72 | 60 |
| | 0.36 | 6.49 | 9.18 | 41 |
| $N{:}P_{cell}$ | 0.74 | 14.65 | 18.88 | 29 |
| | 0.60 | 15.84 | 19.13 | 21 |
| | 0.47 | 16.32 | 19.58 | 20 |
| | 0.36 | 16.59 | 18.45 | 11 |
| $C{:}P_{cell}$ | 0.74 | 87.70 | 145.22 | 66 |
| | 0.60 | 99.02 | 158.31 | 60 |
| | 0.47 | 110.34 | 169.7 | 54 |
| | 0.36 | 113.21 | 162.26 | 43 |

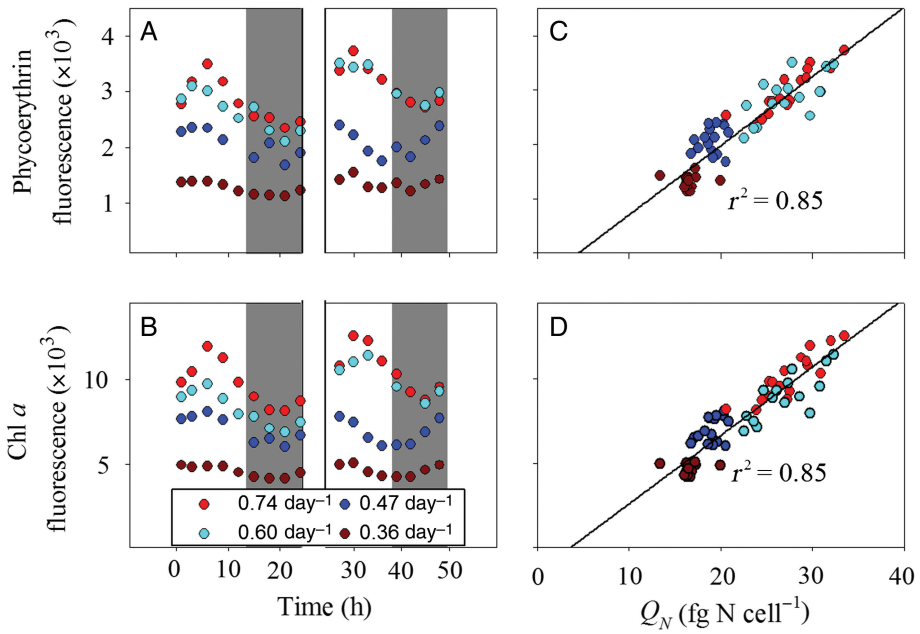


**Fig. 4.** Diel cycling of phycoerythrin (**A**) and Chl *a* (**B**) fluorescence of *Synechococcus* as a function of steady-state growth in nitrate-limited chemostat cultures of *Synechococcus*. Relationships between $Q_N$ and pigment fluorescence are plotted with linear least-squares regression fits (**C** and **D**). Gray bands indicate dark periods during two 24 h periods. Break in *x*-axis denotes 7-day period between first and second 24 h sampling period.

## DISCUSSION

The plasticity in cellular quotas between light and dark periods resulted in pronounced deviation from Redfield stoichiometry. Consistent with previous work showing the accumulation of glycogen throughout light periods and subsequent use to maintain essential chemical processes throughout dark periods (Smith, 1983), $Q_C$ varied substantially during each 24 h period and was synchronized with the 14:10 light–dark cycle. In addition, $Q_C$ was positively related to the growth rate and significantly correlated with cell size, as documented previously (Garcia *et al.*, in review). Because of lower fluctuations in $Q_N$ and $Q_P$ (Fig. 1B), $N$:$P_{cell}$ was not highly variable (Fig. 3E) and $Q_C$ was responsible for the majority of the diel variation in $C$:$N_{cell}$ and $C$:$P_{cell}$ in *Synechococcus* (Fig. 3D and F).

Due to their small cell size, *Synechococcus* is expected to have relatively limited diel variation in elemental stoichiometry (Talmy *et al.*, 2014). When averaged over the diurnal cycle, *Synechococcus* $C$:$N_{cell}$ and $C$:$P_{cell}$ do indeed vary over a relatively limited range [e.g. $C$:$N_{cell}$ between approximately 6 and 8 (by moles) and $C$:$P_{cell}$ between approximately 100 and 140] in comparison to that observed in other, nutrient-limited eukaryotes (e.g. $C$:$N_{cell}$ between approximately 6 and 20 and $C$:$P_{cell}$ between approximately 100 and 600; Caperon and Meyer, 1972; Laws and Wong, 1978; Laws and Bannister, 1980; Elrifi and Turpin, 1985; Geider *et al.*, 1998). Surprisingly, however, *Synechococcus* does have high diurnal variation in $C$:$N_{cell}$ and $C$:$P_{cell}$ (Fig. 3), similar to variable elemental stoichiometry in $N_2$-fixing cyanobacteria, which temporally separate C and $N_2$ fixation between light and dark periods (Mohr *et al.*, 2010; Dron *et al.*, 2012). This relationship among $Q_C$, cell size and growth rate has consequences not only for field measurements of stoichiometry, but also for growth rates, as diel variability in cell size has been used to estimate growth rates of *Synechococcus* (Hunter-Cevera *et al.*, 2014).

As suggested by previous modeling and empirical studies (Pirt, 1982; Vincent, 1992; Clark *et al.*, 2002; Flynn *et al.*, 2002), we suspect that the temporal decoupling of cellular N and P from C ($Q_C$ peaks are separated from $Q_N$ and $Q_P$ peaks by several hours; Fig. 1) could be due in part to the utilization of accumulated carbon reserves (Fig. 1A) to drive N and P uptake during the dark hours, particularly when cells are growing fast. Although some data suggest that nitrate uptake in *Synechococcus* is restricted to the light period (Paerl *et al.*, 2012), the growth rate differential could modulate light and dark uptake of nitrate. For example, although slow-growing cells may rely on the energetically favorable day-time N acquisition, fast-growing cells may need to acquire N during the day and during the night to keep up with the high N demand. Certainly, the growth rate differential is responsible for modulating utilization of different N sources in other organisms within cyanobacteria that fix $N_2$ (Garcia and Hutchins, 2014), a trade-off that is also thought to be thermodynamically controlled. Just as other organisms within cyanobacteria (such as *Crocosphaera*) rely on carbon reserves to supply energy needed to assimilate $N_2$ during the dark period, we recognize the possibility that *Synechococcus* acquires nitrate during the dark period when the N demand for growth is high. The pre-dawn rise in $Q_N$ and $Q_P$ could be associated with dark N and P acquisition, and our model parameterizes the associated energy costs as respiration of reserve carbon (Supplementary data, Equation S3). This perspective presumes that stoichiometric variation within phytoplankton could depend on the thermodynamics of nutrient assimilation. For example, ammonium assimilation is presumed to use less energy relative to nitrate assimilation, possibly influencing stored carbon utilization rates. Thus, the temporal decoupling of $Q_C$, $Q_N$ and $Q_P$ could result from combined effects of timing in cell division and nutrient acquisition and may depend on nutrient source.

Previous models of elemental stoichiometry have assumed that the carbon loss rate is dependent primarily on the growth rate, with other carbon losses negligible (Geider *et al.*, 1998; Pahlow, 2005; Bonachela *et al.*, 2012; Talmy *et al.*, 2014). Using this assumption, the model was able to reproduce the general bimodal pattern in $C$:$N_{cell}$ and $C$:$P_{cell}$ that emerges over our sampling periods (Fig. 3A and C), but fails to adequately reproduce the amplitude of fluctuation in different dilution rates. When it was assumed that dark-period carbon losses are high ($4.0\ day^{-1}$), however, the model was able to reproduce the full amplitude of diurnal changes in $C$:$N_{cell}$ and $C$:$P_{cell}$ (Fig. 3D and F). The improved model fits suggest that *Synechococcus* purges carbon at night, through either respiration or excretion.

We suggest three possible mechanisms describing how *Synechococcus* might benefit from purging excess carbon. The first is that carbon accumulated during the light period is used as energy for respiratory costs associated with repair of core functional apparatus that may have been damaged during the photoperiod (Raven, 1989; Long *et al.*, 1994; Vasilikiotis and Melis, 1994; Talmy *et al.*, 2013; Talmy *et al.*, 2014). The second possibility is related to cell size. In the oligotrophic gyres, there is strong evolutionary pressure to optimize the surface-area-to-volume ratio through small cell size (Clark *et al.*, 2013). Excess carbon in the form of carbohydrate and lipids may take up valuable space within the cell. *Synechococcus* may have evolved a night-time carbon excretion mechanism to enable it to shrink to the smallest possible size, even when growth in a high-light environment necessitates the accumulation of excess carbohydrates. Finally, the mechanism could be important for ocean ecosystem

functioning, as excretion of energy-rich carbon polymers is likely to play a role in algal-heterotrophic interactions (Grossart and Simon, 2007). Excretion of carbon polymers could stimulate bacterial growth and increase nutrient remineralization rates—a potentially crucial adaptation to chronic nutrient limitation.

In addition to cell quotas and elemental ratios, we also observed oscillation in pigment fluorescence (Fig. 3A and B). Although $Q_C$ and cell size are directly linked to light availability (Vaulot *et al.*, 1995; Sato *et al.*, 2015) and co-oscillate in our data (Figs 1 and 2), the variation in pigment fluorescence is more tightly correlated with variation in $Q_N$ (Fig. 4C and D). Pigments change over a diel cycle in natural phytoplankton populations (Sester *et al.*, 1982; Sato *et al.*, 2015), and phycoerythrin is known to be a nitrogen storage compound in *Synechococcus* (Wyman *et al.*, 1985; Yeh *et al.*, 1986).

Diel patterns in elemental stoichiometry may also be linked to patterns in gene expression of different proteins (Stöckel *et al.*, 2011; Mella-Flores *et al.*, 2012; Diamond *et al.*, 2015). However, the large variation in $C{:}N_{cell}$ and $C{:}P_{cell}$ data indicates that $Q_C$ is dominant whereas $Q_N$ and $Q_P$ are minor drivers. This leaves few candidate molecules for driving diel patterns in elemental ratios, and direct measurements of glycogen have been shown to cycle throughout the day in other cyanobacteria (Saito *et al.*, 2011). The relatively invariable $N{:}P_{cell}$ suggests that nucleic acids may be responsible for the minor variation in $Q_N$ and $Q_P$ as proteins do not typically contain a large quantity of P. Cellular nucleic acids are known to increase in response to growth (Churchward *et al.*, 1982; Sterner and Elser, 2002; Garcia *et al.*, in review) and cycle with a daily rhythm (Vaulot *et al.*, 1995). Direct measurements of specific compounds are needed, however, especially as there are no data describing diel patterns in phytoplankton polyphosphates.

## CONCLUSION

Our data show pronounced diel oscillations in the elemental quotas of *Synechococcus* with variability largely depending on the growth rate (Figs 1 and 3) and carbon accumulation driving the majority of variable $C{:}P_{cell}$ and $C{:}N_{cell}$ ratios. The variability in $C{:}N_{cell}$ is larger than expected based on models of variability among phytoplankton groups, but still smaller than the variability observed in large eukaryotic phytoplankton. Our model suggests that *Synechococcus* purges excess carbon during the dark period of a 24 h cycle. The variability observed over a single day is comparable to that over large-scale environmental regimes and should be further investigated in the field for its implications on modeling biogeochemical processes. Differences in diel stoichiometric variability between groups of large and small phytoplankton may contribute to competitive niches within large biogeographical domains.

## SUPPLEMENTARY DATA

Supplementary data can be found online at http://plankt.oxfordjournals.org

## FUNDING

We would like to thank the University of California, Irvine Undergraduate Research Opportunities Program (J.S.L.), the University of California, Irvine Chancellor's ADVANCE Postdoctoral Fellowship Program (N.S.G.), the Gordon and Betty Moore Foundation (GBMF3778) to M. J. Follows (D.T.) and the National Science Foundation Dimensions of Biodiversity (OCE-1046297) and Major Research Instrumentation programs (OCE-1126749) (A.C.M.) for supporting the research presented here.

## REFERENCES

Anning, T., MacIntyre, H. L., Pratt, S. M., Sammes, P. J., Gibb, S. and Geider, R. J. (2000) Photoacclimation in the marine diatom *Skeletonema costatum*. *Limnol. Oceanogr.*, **45**, 1807–1817.

Berman-Frank, I., Quigg, A., Finkel, Z. V., Irwin, A. J. and Haramaty, L. (2007) Nitrogen-fixation strategies and Fe requirements in cyanobacteria. *Limnol. Oceanogr.*, **52**, 2260–2269.

Bertilsson, S., Berglund, O., Karl, D. M. and Chisolm, S. W. (2003) Elemental composition of marine *Prochlorococcus* and *Synechococcus*: implications for the ecological stoichiometry of the sea. *Limnol. Oceanogr.*, **48**, 1721–1731.

Bonachela, J. A., Raghib, M. and Levin, S. A. (2012) Dynamic model of flexible phytoplankton nutrient uptake. *Proc. Natl Acad. Sci. USA*, **109**, 3190–3190.

Caperon, J. and Meyer, J. (1972) Nitrogen-limited growth of marine phytoplankton I. Changes in population characteristics with steady-state growth rate. *Deep Sea Res.*, **19**, 601–618.

Churchward, G., Bremer, H. and Young, R. (1982) Macromolecular composition of bacteria. *J. Theor. Biol.*, **94**, 651–670.

Clark, J. R., Flynn, K. J. and Owens, N. J. P. (2002) The large capacity for dark nitrate-assimilation in diatoms may overcome nitrate limitation of growth. *New Phytol.*, **155**, 101–108.

Clark, J. R., Lenton, T. M., Williams, H. T. P. and Daines, S. J. (2013) Environmental selection and resource allocation determine spatial patterns in picophytoplankton cell size. *Limnol. Oceanogr.*, **58**, 1008–1022.

Deutsch, C., Gruber, N. and Key, R. M. (2001) Denitrification and $N_2$ fixation in the Pacific Ocean. *Global Biogeochem. Cycles*, **15**, 483–506.

Deutsch, C., Sarmiento, J. L., Sigman, D. M., Gruber, N. and Dunne, J. P. (2007) Spatial coupling of nitrogen inputs and losses in the ocean. *Nature*, **445**, 163–167.

DeVries, T. and Deutsch, C. (2014) Large-scale variations in the stoichiometry of marine organic matter respiration. *Nat. Geosci.*, **7**, 890–894.

Diamond, S., Jun, D., Rubin, B. E. and Golden, S. S. (2015) The circadian oscillator in *Synechococcus elongatus* controls metabolite partitioning during diurnal growth. *Proc. Natl Acad. Sci. USA*, **112**, 1916–1925.

Dron, A., Rabouille, S., Claquin, P., Le Roy, B., Talec, A. and Sciandra, A. (2012) Light-dark (12:12) cycle of carbon and nitrogen metabolism in *Crocosphaera watsonii* WH8501: relation to the cell cycle. *Environ. Microbiol.*, **14**, 967–981.

Elrifi, I. R. and Turpin, D. H. (1985) Steady state luxury consumption and the concept of optimum nutrient ratios: a study with phosphate and nitrate limited selenatrum (*chlorophyta*). *J. Phycol.*, **21**, 592–602.

Flombaum, P., Gallegos, J. L., Gordillo, R. A., Rincon, J., Zabala, L. L., Jiao, N., Karl, D. M., Li, W. K. W. *et al.* (2013) Present and future global distributions of the marine Cyanobacteria *Prochlorococcus* and *Synechococcus*. *Proc. Natl Acad. Sci. USA*, **110**, 9824–9829.

Flynn, K. J. (2008) Use, abuse, misconceptions and insights from quota models—the droop cell quota model 40 years on. *Oceanogr. Mar. Biol.*, **46**, 1–23.

Flynn, K. J., Clark, D. R. and Owens, N. J. P. (2002) Modeling suggests that optimization of dark nitrogen-assimilation need not be a critical selective feature in phytoplankton. *New Phytol.*, **155**, 109–119.

Garcia, N. S., Bonachela, J. A. and Martiny, A. C. (in review) Interactions between growth-dependent cell size, nutrient availability and cellular elemental stoichiometry of marine *Synechococcus*.

Garcia, N. S. and Hutchins, D. A. (2014) Light-limited growth rate modulates nitrate inhibition of dinitrogen fixation in the marine cyanobacterium *Crocosphaera watsonii*. *PLoS ONE*, **9**, e114465.

Geider, R. J. and La Roche, J. (2002) Redfield revisited: variability of C:N:P in marine microalgae and its biochemical basis. *Eur. J. Phycol.*, **37**, 1–17.

Geider, R. J., MacIntyre, H. J. and Kana, T. M. (1998) A dynamic regulatory model of phytoplankton acclimation to light, nutrients and temperature. *Limnol. Oceanogr.*, **43**, 679–694.

Gradoville, M. R., White, A. E. and Letelier, R. M. (2014) Physiological response of *Crocosphaera watsonii* to enhanced and fluctuating carbon dioxide conditions. *PLoS ONE*, **9**, e110660.

Granum, E., Kirkvold, S. and Myklestad, S. M. (2002) Cellular and extracellular production of carbohydrates and amino acids by the marine diatom *Skeletonema costatum*: diel variations and effects of N depletion. *Mar. Ecol. Prog. Ser.*, **242**, 83–94.

Grossart, H. P. and Simon, M. (2007) Interactions of planktonic algae and bacteria: effects on algal growth and organic matter dynamics. *Aquatic Microb. Ecol.*, **47**, 163–176.

Heldal, M., Scanlan, D. J. and Norland, S. (2003) Elemental composition of single cells of various strains of marine *Prochlorococcus* and *Synechococcus* using X-ray microanalysis. *Limnol. Oceanogr.*, **48**, 1732–1743.

Ho, T. Y., Quigg, A., Finkel, Z. V., Milligan, A. J., Wyman, K., Falkowski, P. G. and Morel, F. M. M. (2003) The elemental composition of some marine phytoplankton. *J. Phycol.*, **39**, 1145–1159.

Hunter-Cevera, K. R., Neubert, M. G., Solow, A. R., Olson, R. J., Shalapyonok, A. and Sosik, H. M. (2014) Diel size distributions reveal seasonal growth dynamics of a coastal phytoplankter. *Proc. Natl Acad. Sci. USA*, **111**, 9852–9857.

Jacquet, S., Partensky, F., Lennon, J. F. and Vaulot, D. (2001) Diel patterns of growth and division in marine picoplankton in culture. *J. Phycol.*, **37**, 357–369.

Karl, D.M., Björkman, K. M., Dore, J. E., Fujieki, L., Hebel, D. V., Houlihan, T., Letelier, R. and Tupas, L. M. (2001) Ecological nitrogen-to-phosphorus stoichiometry at station ALOHA. *Deep Sea Res. Part II*, **48**, 1529–1566.

Krishnamurthy, A., Moore, J. K., Mahowald, N. and Luo, S. (2009) Impacts of increasing anthropogenic soluble iron and nitrogen deposition on ocean biogeochemistry. *Global Biogeochem. Cy.*, **23**, GB3016.

Laws, E. A. and Bannister, T. T. (1980) Nutrient- and light-limited growth of *Thalassiosira fluviatilis* in continuous culture, with implications for phytoplankton growth in the ocean. *Limnol. Oceanogr.*, **25**, 457–473.

Laws, E. A. and Wong, D. C. L. (1978) Studies of carbon and nitrogen metabolism by three marine phytoplankton species in nitrate-limited continuous culture. *J. Phycol.*, **7**, 406–417.

Long, S. P., Humphries, S. and Falkowski, P. G. (1994) Photoinhibition of photosynthesis in nature. *Annu. Rev. Plant Biol.*, **45**, 633–662.

Mackey, K. R. M., Paytan, A., Caldeira, K., Grossman, A. R., Moran, D., McIlvin, M. and Saito, M. A. (2013) Effect of temperature on photosynthesis and growth in marine *Synechococcus* spp. *Plant Physiol.*, **163**, 815–829.

Martin, J. H., Knauer, G. A., Karl, D. M. and Broenkow, W. W. (1987) VERTEX: carbon cycling in the northeast Pacific. *Deep-Sea Res. Part I*, **34**, 267–285.

Martiny, A. C., Pham, C. T. A., Primeau, F. W., Vrugt, J. A., Moore, J. K., Levin, S. A. and Lomas, M. W. (2013a) Strong latitudinal patterns in the elemental ratios of marine plankton and organic matter. *Nat. Geosci.*, **6**, 279–283.

Martiny, A. C., Vrugt, J. A., Primeau, F. W. *et al.* (2013b) Regional variation in the particulate organic carbon to nitrogen ratio in the surface ocean. *Global Biogeochem. Cy.*, **27**, 723–731.

Mary, I., Garczarek, L., Tarran, G. A., Kolowrat, C., Terry, M. J., Scanlan, D. J., Burkill, P. H. and Zubkov, M. V. (2008) Diel rhythmicity in amino acid uptake by *Prochlorococcus*. *Environ. Microbiol.*, **10**, 2124–2131.

Matallana-Surget, S., Derock, J., Leroy, B., Badri, H., Deschoenmaeker, F. and Wattiez, R. (2014) Proteome-wide analysis and diel proteomic profiling of the cyanobacterium *Arthrospira platensis* PCC 8005. *PLoS ONE*, **9**, e0099076.

McCarthy, J. and Goldman, J. C. (1979) Nitrogenous nutrition of marine phytoplankton in nutrient-depleted waters. *Science*, **203**, 670–672.

Mella-Flores, D., Six, C., Ratin, M., Partensky, F., Boutte, C., Le Corquille, G., Marie, D., Blot, N. *et al.* (2012) *Prochlorococcus* and *Synechococcus* have evolved different adaptive mechanisms to cope with light and UV stress. *Front. Microbiol.*, **3**, 1–20.

Michaels, A., Dow, R. and Elardo, K. (1997a) *The Determination of Phosphorus in Seawater*, in: Bermuda Atlantic Time-series Study Methods, St. George's, Bermuda, pp. 71–74.

Michaels, A., Dow, R. and Howse, F. (1997b) *The Determination of Nitrate in Seawater*, in: Bermuda Atlantic Time-series Study Methods, St. George's, Bermuda, pp. 61–66.

Mohr, W., Intermaggio, M. P. and LaRoche, J. (2010) Diel rhythm of nitrogen and carbon metabolism in the unicellular, diazotrophic cyanobacterium *Crocosphaera watsonii* WH8501. *Environ. Microbiol.*, **12**, 412–421.

Moore, L. R., Goericke, R. and Chisholm, S. W. (1995) Comparative physiology of Synechococcus and Prochlorococcus: influence of light and temperature on growth, pigments, fluorescence, and absorptive properties. *Mar. Ecol. Prog. Ser.*, **116**, 259–275.

Mouginot, C., Zimmerman, A. E., Bonachela, J. A., Fredricks, H., Allison, S. D., Van Mooy, B. A. S. and Martiny, A. C. (2015) Resource allocation by the marine cyanobacterium *Synechococcus* WH8102 in response to different nutrient supply ratios. *Limnol. Oceanogr.*, **60**, 1634–1641.

Paerl, R. W., Tozzi, S., Kolber, Z. S. and Zehr, J. P. (2012) Variation in the abundance of *Synechococcus SP.* CC9311 *nar*B mRNA relative to changes in light, nitrogen growth conditions and nitrate assimilation. *J. Phycol.*, **48**, 1028–1039.

Pahlow, M. (2005) Linking chlorophyll—nutrient dynamics to the Redfield N:C ratio with a model of optimal phytoplankton growth. *Mar. Ecol. Prog. Ser.*, **287**, 33–43.

Pirt, S. J. (1982) Maintenance energy: a general model for energy-limited and energy sufficient growth. *Arch. Microbiol.*, **133**, 300–302.

Prézelin, B. B. (1992) Diel periodicity in phytoplankton productivity. *Hydrobiologia*, **238**, 1–35.

Quigg, A., Irwin, A. J. and Finkel, Z. V. (2011) Evolutionary inheritance of elemental stoichiometry in phytoplankton. *Proc. Biol. Sci.*, **278**, 526–534.

Raven, J. A. (1989) Fight or flight: the economics of repair and avoidance of photoinhibition of photosynthesis. *Funct. Ecol.*, **3**, 5–19.

Redfield, A. C. (1958) The biological control of chemical factors in the environment. *Am. Sci.*, **46**, 205–221.

Rhee, G. Y. (1978) Effects of N:P atomic ratios nitrate limitation on algal growth, cell composition, nitrate uptake. *Limnol. Oceanogr.*, **23**, 10–25.

Saito, M. A., Bertrand, E. M., Dutkiewicz, S., Bulygin, V. V., Moran, D. M., Monteiro, F. M, Follows, M. J., Valois, F. W. *et al.* (2011) Iron conservation by reduction of metalloenzyme inventories in the marine diazotroph *Crocosphaera watsonii*. *Proc. Natl Acad. Sci. USA*, **108**, 2184–2189.

Sato, M., Kodama, T., Hashihama, F. and Furuya, K. (2015) The effects of diel cycles and temperature on size distributions of pico-and nanophytoplankton in the subtropical and tropical Pacific Ocean. *Plankt. Benthos Res.*, **10**, 26–33.

Sester, P. J., Guinasso, N. L. J. and Schink, D. R. (1982) Daily patterns of fluorescence *in vivo* in the central equatorial ocean. *J. Mar. Res.*, **40**, 453–471.

Smith, A. J. (1983) Modes of cyanobacterial carbon metabolism. *Ann. Microbiol.*, **134B**, 93–113.

Sterner, R. W. and Elser, J. J. (2002) *Biological Stoichiometry: The Biology of Elements From Molecules to the Biosphere*. Princeton University Press, Princeton, New Jersey.

Stöckel, J., Jacobs, J. M., Elvitigala, T. R., Liberton, M., Welsh, E. A., Polpitiya, A. D., Gritsenko, M. A., Nicora, C. D. *et al.* (2011) Diurnal rhythms result in significant changes in the cellular protein complement in the cyanobacterium *Cyanothece* 51142. *PLoS ONE*, **6**, e0016680.

Talmy, D., Blackford, J., Hardman-Mountford, N. J., Dumbrell, A. J. and Geider, R. J. (2013) An optimality model of photoadaptation in contrasting aquatic light regimes. *Limnol. Oceanogr.*, **58**, 1802–1818.

Talmy, D., Blackford, J., Hardman-Mountford, N. J., Polimene, L., Follows, M. J. and Geider, R. J. (2014) Flexible C:N ratio enhances metabolism of large phytoplankton when resource supply is intermittent. *Biogeoscience*, **11**, 4881–4895.

Teng, Y.-C., Primeau, F. W., Moore, J. K., Lomas, M. W. and Martiny, A. C. (2014) Global-scale variations of the ratios of carbon to phosphorus in exported marine organic matter. *Nat. Geosci.*, **7**, 895–898.

Toseland, A., Daines, S. J. and Clark, J. R. (2013) The impact of temperature on marine phytoplankton resource allocation and metabolism. *Nat. Clim. Change*, **3**, 979–984.

Urabe, J., Kyle, M., Makino, W., Yoshida, T., Andersen, T. and Elser, J. J. (2002) Reduced light increases herbivore production due to stoichiometric effects of light/nutrient balance. *Ecology*, **83**, 619–627.

Van Oijen, T., Van Leeuwe, M. A. and Gieskes, W. W. C. (2003) Variation of particulate carbohydrate pools over time and depth in a diatom-dominated plankton community at the Antarctic Polar Front. *Polar Biol.*, **26**, 195–201.

Vasilikiotis, C. and Melis, A. (1994) Photosystem II reaction center damage and repair cycle: chloroplast acclimation strategy to irradiance stress. *Proc. Natl Acad. Sci. USA*, **91**, 7222–7226.

Vaulot, D., Marie, D., Olson, R. J. and Chisholm, S. W. (1995) Growth of *Prochlorococcus*, a photosynthetic prokaryote, in the equatorial Pacific Ocean. *Science*, **268**, 1480–1482.

Vincent, W. F. (1992) The daily pattern of nitrogen uptake by phytoplankton in dynamic mixed layer environments. *Hydrobiologia*, **238**, 37–52.

Weber, T. S. and Deutsch, C. (2010) Ocean nutrient ratios governed by plankton biogeography. *Nature*, **467**, 550–554.

Wyman, M., Gregory, R. P. and Carr, N. G. (1985) Novel role for phycoerythrin in a marine Cyanobacterium, *Synechococcus* strain DC2. *Science*, **230**, 818–820.

Yeh, S. W., Ong, L. J. and Glazer, A. N. (1986) Role of phycoerythrin in marine picoplankton *Synechococcus* spp. *Science*, **234**, 1422–1423.